

Disentanglement of magnetic contributions in multi-component systems by using X-ray magnetic circular dichroism at a single absorption edge

Jesús Chaboy,^{a*} María Ángeles Laguna-Marco,^b Cristina Piquer,^c Roberto Boada,^a Hiroshi Maruyama^d and Naomi Kawamura^e

^aInstituto de Ciencia de Materiales de Aragón and Departamento de Física de la Materia Condensada, CSIC-Universidad de Zaragoza, 50009 Zaragoza, Spain, ^bAdvanced Photon Source, Argonne National Laboratory, Argonne, IL 60439, USA, ^cInstituto de Ciencia de Materiales de Aragón and Departamento de Ciencia y Tecnología de Materiales y Fluidos, CSIC-Universidad de Zaragoza, 50009 Zaragoza, Spain, ^dGraduate School of Science, Hiroshima University, 1-3-1 Kagamiyama, Higashi-Hiroshima 739-8526, Japan, and ^eJapan Synchrotron Radiation Research Institute/SPring-8, 1-1-1 Kouto, Sayo, Hyogo 679-5198, Japan. E-mail: jchaboy@unizar.es

X-ray magnetic circular dichroism (XMCD) has become in recent years an outstanding tool for studying magnetism. Its element specificity, inherent to core-level spectroscopy, combined with the application of magneto-optical sum rules allows quantitative magnetic measurements at the atomic level. These capabilities are now incorporated as a standard tool for studying the localized magnetism in many systems. However, the application of XMCD to the study of the conduction-band magnetism is not so straightforward. Here, it is shown that the atomic selectivity is not lost when XMCD probes the delocalized states. On the contrary, it provides a direct way of disentangling the magnetic contributions to the conduction band coming from the different elements in the material. This is demonstrated by monitoring the temperature dependence of the XMCD spectra recorded at the rare-earth L_2 -edge in the case of RT_2 (R = rare-earth, T = $3d$ transition metal) materials. These results open the possibility of performing element-specific magnetometry by using a single X-ray absorption edge.

Keywords: X-ray magnetic circular dichroism; atom-specific magnetometry.

1. Introduction

The possibility of disentangling the magnetic contribution of different atomic species within the same material has been a challenge for a long time. Most of the experimental techniques aimed at studying the magnetic properties of materials are sensitive to the total magnetization of the measured system and, consequently, they cannot discern between the contributions of different atoms in the material. Within this scenario, X-ray magnetic circular dichroism (XMCD), the difference in absorption of left- and right-circularly polarized X-rays by a magnetized sample, emerges as an outstanding tool for studying magnetism by incorporating the element specificity of core-level spectroscopies (Funk *et al.*, 2005; Lovesey & Collins, 1996; Stöhr, 1999).

The advantage of X-rays over optical techniques such as the Kerr effect lies in the fact that the absorption edges from a core level have energies which are characteristic for each element and, owing to the dipole selection rules, final states with different symmetries can be probed by choosing the initial state. In this way, as each element can be probed

separately by appropriately choosing the absorption edge, XMCD opens the possibility of performing element-specific magnetic hysteresis measurements (Chen *et al.*, 1993), magnetic domain imaging *etc.* (Kortright *et al.*, 1999). However, while the capabilities of XMCD are squeezed in the case of localized states carrying a magnetic moment [f -states of lanthanides and actinides ($M_{4,5}$ -edges), d -states of transition metals ($L_{2,3}$)], the same does not hold when the delocalized states are being probed. While atomic calculations reproduce quantitatively the XMCD signal in the soft X-ray range, the theoretical description is more difficult to handle in the hard X-ray domain (Schütz *et al.*, 1987, 1988; Wang *et al.*, 1993; Harmon & Freeman, 1974). As a consequence, most of these selective magnetometry experiments are limited to the soft X-ray energy in which the surface sensitivity may affect the magnetic characterization of the samples. Moreover, in the case of materials containing both transition metal and heavier elements such as lanthanides or noble metals, the XMCD characterization of these heavy elements has to be performed in the hard X-ray region which implies a dramatic change of the probing depth. As a consequence, the magnetic properties

of the different components of the material cannot be obtained under the same experimental conditions. This scenario leads us to look for a new experimental method aimed at obtaining the magnetic characterization of complex magnetic systems by using XMCD in the hard X-ray region. The fact that the energy of the X-rays is raised from the soft to the hard X-ray region has the main advantages of avoiding surface effects, of guaranteeing that the XMCD becomes a real bulk probe and, in addition, the flexibility of the sample environment is enhanced allowing studies under extreme conditions of temperature, applied magnetic field and applied pressure (Ishimatsu *et al.*, 2007).

We have performed in the past a systematic study of rare-earth (R) and transition metal (T) R–T compounds by means of XMCD at the *L*-edges and the *K*-edge of rare-earth and the transition metals, respectively. By recording the XMCD at these absorption edges, the conduction-band *4p* states of transition metals and the *5d* states of rare-earths are probed. These delocalized states propagate the magnetic interaction between the R-*4f* and T-*3d* electrons coupling the magnetic properties of both magnetic sublattices and determining the magnetic behaviour of the material. We and others have shown in previous works that in the case of multi-component magnetic systems such as R–T intermetallics both atomic species influence the XMCD spectra recorded at the *L*₂-edge¹ of the rare-earth (Laguna-Marco, 2007; Laguna-Marco *et al.*, 2005*a,b*, 2008*a,b*; Giorgetti *et al.*, 2004; Chaboy *et al.*, 2007*b*; Ishimatsu *et al.*, 2007) and at the *K*-edge of the transition metal (Laguna-Marco *et al.*, 2005*a*; Ishimatsu *et al.*, 2007; Chaboy *et al.*, 1996, 1998*b*, 2004, 2007*a,c*; Rueff *et al.*, 1998). These experimental results have been accounted for in terms of the R(*5d*)–T(*d*) hybridization (Laguna-Marco *et al.*, 2008*a*; Chaboy *et al.*, 2007*b*). Therefore, despite the atomic selectivity inherent to the X-ray absorption, the transition metal also contributes to the rare-earth XMCD spectra and, conversely, there is a non-negligible contribution of the lanthanide metal to the *K*-edge XMCD spectra of the transition metal. Beyond this, information is of fundamental importance in order to obtain a correct interpretation of the R *L*₂- and T *K*-edge XMCD signals; it also opens the possibility of disentangling the magnetic contribution of different atomic species within the same material by using a single X-ray absorption edge.

In this way we show here that, when a delocalized final state is probed by the absorption process, XMCD is a simultaneous fingerprint of both the rare-earth and the transition metal even when only a single absorption edge of an atomic element is tuned. This does not mean that the atomic selectivity is lost. On the contrary, it provides the possibility of studying at the same time the magnetic behaviour of different magnetic species. In particular, by tuning the X-ray absorption either at the *L*₂-edge of the rare-earth or at the *K*-edge of the transition metal, it is possible to disentangle, using only this edge, the magnetization of both rare-earth and transition metal. This is

shown here in the case of different RFe₂ and RCo₂ compounds through the temperature regime between 4.2 K and room temperature. The main advantages of this new method of performing atom-specific magnetometry by using a single X-ray absorption edge lie in the fact that the magnetic characterization of the different elements is obtained exactly under the same experimental conditions. Moreover, this being a hard X-ray method, it avoids all the inherent difficulties of using soft X-rays and it broadens the experimental conditions especially regarding the possibility of performing the magnetic characterization under applied pressure.

2. Experimental

ErAl₂, ErCo₂, ErFe₂, Er(Fe_{0.75}Al_{0.25})₂, Er(Fe_{0.5}Al_{0.5})₂, HoCo₂ and HoAl₂ samples were prepared by arc-melting the pure elements under Ar protective atmosphere. The ingots were annealed at 1123 K for one week. Structural characterization was performed at room temperature by means of powder X-ray diffraction by using a rotating-anode Rigaku diffractometer in the Bragg–Brentano geometry, with Cu *K* α radiation. All the samples are single phase and show the MgCu₂-type (C15) Laves structure (Laguna-Marco, 2007). The macroscopic magnetic measurements were performed following standard methods in magnetic fields up to 50 kOe, by using a commercial SQUID magnetometer (Quantum Design MPMS-S5).

XMCD experiments were performed at beamline BL39XU of the SPring-8 facility (Maruyama, 2001). XMCD spectra were recorded in transmission mode at the rare-earth *L*_{2,3}-edges by using the helicity-modulation technique (Suzuki *et al.*, 1998). The sample is magnetized by an external magnetic field applied in the direction of the incident beam and the helicity is changed from positive to negative each energy point. The XMCD spectrum corresponds to the spin-dependent absorption coefficient obtained as the difference of the absorption coefficient $\mu_c = (\mu^- - \mu^+)$ for antiparallel, μ^- , and parallel, μ^+ , orientation of the photon helicity and the magnetic field applied to the sample. For the sake of accuracy, the direction of the applied magnetic field is reversed and XMCD, now $\mu_c = (\mu^+ - \mu^-)$, is recorded again by switching the helicity. The subtraction of the XMCD spectra recorded for both field orientations cancels, if present, any spurious signal.

For the measurements, homogeneous layers of the powdered samples were made by spreading fine powders of the material on adhesive tape. The thickness and homogeneity of the samples were optimized to obtain the best signal-to-noise ratio. The XMCD spectra were recorded at *T* = 5 K and $\mu_0 H$ = 5 T. In all cases the origin of the energy scale was chosen at the inflection point of the absorption edge, *E*₀ (9263 and 8918 eV for the Er and Ho *L*₂-edge, respectively). Consequently, all the comparisons are referred to the *E* – *E*₀ scale. The XAS spectra were normalized to the averaged absorption coefficient at high energy (*E* – *E*₀ \simeq 50 eV).

¹ While the effect of the magnetism of the transition metal is notorious in the *L*₂-edge XMCD spectra, no significant effect is detected in the XMCD recorded at the Er *L*₃-edge. A detailed discussion can be found by Chaboy *et al.* (2007*b*).

3. Results and discussion

The rare-earth L_2 -edge XMCD spectra of ErAl_2 and HoAl_2 recorded at $T = 5$ K are shown in Fig. 1. In both cases the spectral profile consists of a main negative peak (A) at ~ 1 eV above the edge and a positive structure (B) located at ~ 7 eV above the edge. In addition, the ratio of the intensity of these main peaks is also the same, $I_A/I_B \simeq -3$, in both the Er and Ho L_2 XMCD spectra. Moreover, both absorption edges show a shoulder-like feature at the low-energy side of the main negative peak. This feature is due to a quadrupolar ($2p \rightarrow 4f$) transition that accompanies the main dipolar ($2p \rightarrow 5d$) transitions at the L_2 -edge (Chaboy *et al.*, 1998a). The simul-

taneous presence of both quadrupolar and dipolar transitions (Carra *et al.*, 1991; Lang *et al.*, 1995) and the need to include the $4f$ - $5d$ intra-atomic exchange interaction (Jo & Imada, 1993; Matsuyama *et al.*, 1997; van Veenendaal *et al.*, 1997) points out the crucial role of the $4f$ electrons in determining the L_2 -edge XMCD even when the empty $5d$ band is probed. Within this framework the similarity of the spectral shape observed for both ErAl_2 and HoAl_2 compounds is in agreement with the atomic-like picture used to account for the XMCD at the rare-earth L -edges (Matsuyama *et al.*, 1997; van Veenendaal *et al.*, 1997). As a consequence, no significant modification of this absorption profile is expected if Al is substituted by a $3d$ metal. Surprisingly, the Er L_2 -edge XMCD

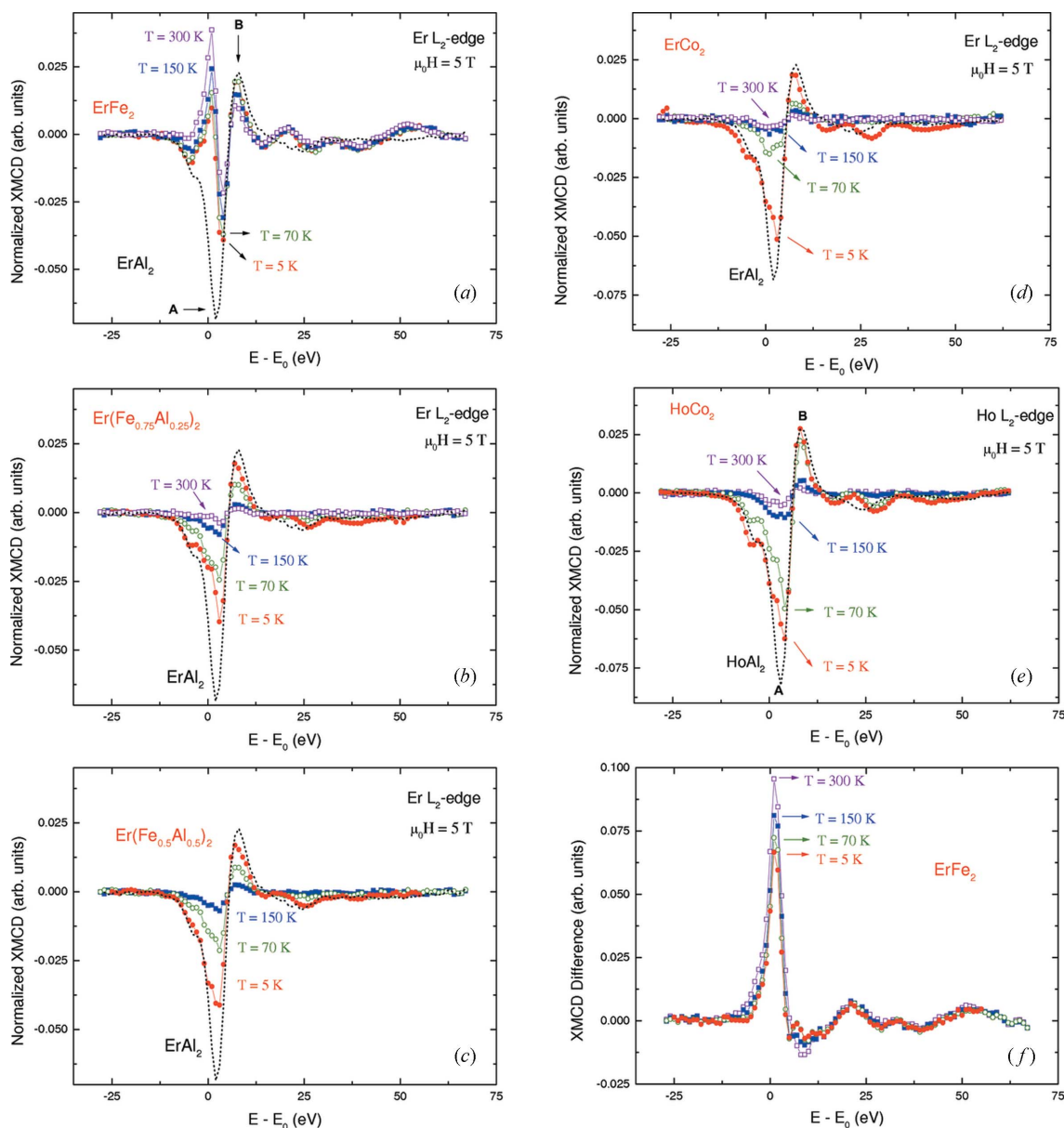


Figure 1 Normalized XMCD spectra recorded at the Er L_2 -edge in (a) ErFe_2 , (b) $\text{Er}(\text{Fe}_{0.75}\text{Al}_{0.25})_2$, (c) $\text{Er}(\text{Fe}_{0.5}\text{Al}_{0.5})_2$ and (d) ErCo_2 , together with those at the Ho L_2 -edge XMCD from HoCo_2 and HoAl_2 (e); $T = 5$ K (red, filled circles), 70 K (green, open circles), 150 K (blue, filled squares) and 300 K (purple, open squares). The dotted line in each panel shows the spectrum from the RAl_2 compound (R = Er and Ho) measured at $T = 5$ K. In all of the cases the applied magnetic field was 5 T. Panel (f) shows the extracted Er L_2 XMCD spectra from ErFe_2 , obtained by subtracting that of ErAl_2 .

spectra recorded through the $\text{Er}(\text{Fe}_x\text{Al}_{1-x})_2$ series are quite different from those of ErAl_2 . A similar modification with respect to the RAl_2 case is observed when Al is substituted by Co in both ErCo_2 and HoCo_2 . When the magnetic (Co or Fe) 3d metal is placed in the RT_2 lattice, both the shape and the amplitude of the negative XMCD contribution at the edge, peak *A*, are modified in comparison with those of RAl_2 . The amplitude of this peak is strongly reduced by factors of $\sim 40\%$ and $\sim 25\%$ for the Fe and Co compounds, respectively, with respect to the RAl_2 case. In addition, the spectral shape evolves from a single negative peak in RAl_2 to a more structured profile showing two components when the 3d metals are present. In this respect, the case of ErFe_2 is of special significance as a positive peak emerges at the energy at which the XMCD spectrum of ErAl_2 shows the negative peak *A*.

This behaviour, showing a different XMCD shape for RT_2 compounds with different transition metal (Al, Fe and Co), cannot be explained in terms of the current knowledge of the rare-earth XMCD signals at the *L*-absorption edges. All these ferromagnetic compounds exhibit the same C15-Laves crystal structure. More importantly, the 4*f* magnetic moments are close to the free-ion values under the working conditions of temperature $T = 5$ K and applied magnetic field $\mu_0 = 5$ T (Laguna-Marco, 2007; Burzo *et al.*, 1990; Purwins *et al.*, 1976). Therefore, it is difficult to account for the observed behaviour in terms of the variation of the 4*f* magnetism or the intra-atomic 4*f*–5*d* interaction through the three series. What is expected is that all these spectra are similar to the XMCD spectra of the RAl_2 compounds as they can be considered as corresponding to a pure rare-earth metal as no magnetism is carried by the Al atoms. The fact that the magnetic properties of the R counterpart (Al, Fe and Co) are clearly different suggests that the origin of such a behaviour stems from an unexpected contribution arising from the T sublattice. According to previous systematic experiences, this contribution is related to the magnetic contribution of the specific transition metal in the compound even when the rare-earth is being probed by the X-rays (Laguna-Marco, 2007; Laguna-Marco *et al.*, 2005*a,b*, 2008*a,b*).

This result suggests that XMCD at the L_2 -edge of the rare-earth in this class of R–T materials is a simultaneous fingerprint of the magnetism of both the rare-earth and the transition metal even when only an atomic element is tuned. The question to answer is whether this peculiarity can also provide quantitative information about the magnetic properties of both sublattices separately. To this end we have studied the dependence on temperature of the XMCD signals recorded at the R- L_2 absorption edge. The behaviour of the temperature dependence of the Er L_2 -edge XMCD spectrum in ErFe_2 is a paradigmatic case. As noted above, a positive peak emerges at the absorption edge and its intensity increases with temperature. This behaviour is not envisaged at all. In principle, one expects that the amplitude of the XMCD signal decreases as temperature increases, reflecting the weakening of the Er magnetic moment as temperature increases. To account for such anomalous behaviour we have considered that the XMCD at the L_2 -absorption edges is not exclusively due to

the rare-earth being probed itself, but there is also a contribution from the neighbouring magnetic transition-metal atoms. In this way the XMCD signal can be decomposed as the addition of two contributions,

$$\text{XMCD}_{\text{RT}_2}(T) = \text{XMCD}_{\text{XMCD}_R}(T) + \text{XMCD}_{\text{XMCD}_T}(T), \quad (1)$$

one exclusively owing to the rare-earth, XMCD_R , and the second owing to the transition metal, XMCD_T . Within the atomic picture discussed above, the rare-earth contribution to the L_2 -edge XMCD spectra is mainly determined by the 4*f* electrons. Because they are close to the free-ion values, we can assume that in the case of the RT_2 compounds the rare-earth XMCD_R contribution to the XMCD spectrum corresponds to the whole XMCD spectrum of the RAl_2 compound as Al atoms do not carry magnetic moment and thus XMCD_T should be zero. Under these assumptions it is possible to isolate the contribution of the transition metal to the R L_2 XMCD by subtracting from each recorded dichroic spectrum that of RAl_2 with the same R, *i.e.* $\text{XMCD}_T = \text{XMCD}_{\text{RT}_2} - \text{XMCD}_{\text{RAl}_2}$. It should be noted that this procedure also cancels any contribution stemming from the atomic-like quadrupolar transition to the R(4*f*) states as these 4*f* states are not affected by the substitution at the T sites.

We show in Fig. 1 the result of applying this procedure in the case of ErFe_2 . Similar results are found in the cases of $\text{Er}(\text{Fe}_{0.75}\text{Al}_{0.25})_2$, $\text{Er}(\text{Fe}_{0.5}\text{Al}_{0.5})_2$, ErCo_2 and HoCo_2 compounds. The extracted XMCD_T contribution shows an intense positive peak at the absorption edge. The profile is basically the same regardless of the rare-earth or the transition metal. Therefore, one can conclude that the contribution of the transition metal to the dichroism of the rare-earth is mainly limited to the absorption edge, *i.e.* to the energy region where the negative peak (*A*) appears, while the higher-energy region, peak *B*, is significantly less affected. For example, in the case of ErFe_2 at 5 K, the intensity of the subtracted signal at the *B* peak is one order of magnitude smaller than at the *A* peak, and it becomes 20 times smaller at room temperature. This result opens the possibility of disentangling the thermal dependence of both contributions from the XMCD spectra: the intensity of peak *B* recorded as a function of temperature should reflect the temperature dependence of the rare-earth sublattice magnetization, $M_R(T)$, while the intensity of peak *A* contains the dependence on temperature of the magnetization of both the rare-earth and transition-metal sublattices. Then, we have derived $M_R(T)$ from the intensity of peak *B* as

$$M_R(T) = M_R(T = 5 \text{ K}) \times \frac{I_B(T)}{I_B(T = 5 \text{ K})}. \quad (2)$$

We have assumed free ion values at low temperature and then $M_R(T = 5 \text{ K})$ equals $9\mu_B$ and $10\mu_B$ for Er and Ho compounds, respectively. The next step in determining the temperature dependence of the transition-metal magnetization, $M_T(T)$, from the rare-earth L_2 -edge XMCD spectrum is to determine the $\text{XMCD}_T(T)$ term from equation (1). To this end we have applied the subtraction method described above, as the dependence in temperature of the pure rare-earth contribution, $\text{XMCD}_R(T)$, should be the same as for the RAl_2

compound. However, the magnetic ordering temperatures of both RT_2 ($T_C \simeq 600$ K) and RAI_2 ($T_C \simeq 13$ K) compounds significantly differ. Thus, it is not possible to identify $XMCD_R(T)$ with $XMCD_{RAI_2}(T)$. For this reason we have considered that $XMCD_R(T)$ is given by the signal recorded at $T = 5$ K for the RAI_2 compound factorized by the reduction of the rare-earth magnetization,

$$XMCD_R(T) = f(T) \times XMCD_{RAI_2}(T = 5 \text{ K}), \quad (3)$$

where $f(T) = M_R(T)/M_R(T = 5 \text{ K})$ has been derived from the temperature dependence of the intensity of peak B according to equation (2). Then, $M_T(T)$ is obtained as

Table 1

Temperature dependence of the magnetization in an applied field of 5 T, M_{Exp} , and that derived from the rare-earth L_2 -edge XMCD spectra, M_{Calc} ; M_R and M_T are the magnetization of the rare-earth and transition-metal sublattices, respectively.

T (K)	M ($\mu_B/f.u.$)	ErFe ₂	Er(Fe _{0.75} Al _{0.25}) ₂	Er(Fe _{0.5} Al _{0.5}) ₂	ErCo ₂	HoCo ₂
5	M_{Exp}	6.00	6.26	6.72	7.65	8.20
	M_{Calc}	6.00	6.26	6.72	7.65	8.2
	M_R	9.00	9.00	9.00	9.00	10.00
	M_T	-3.00	-2.74	-2.28	-1.35	-1.8
70	M_{Exp}	5.50	4.88	3.56	2.18	6.45
	M_{Calc}	5.83	5.13	3.53	2.32	6.43
	M_R	9.12	8.15	5.41	3.07	8.94
	M_T	-3.29	-3.01	-1.88	-0.76	-2.51
150	M_{Exp}	4.03	2.46	0.97	0.86	1.47
	M_{Calc}	3.84	2.44	1.10	1.17	1.88
	M_R	6.90	4.30	1.53	1.65	2.44
	M_T	-3.06	-1.85	-0.44	-0.49	-0.57
300	M_{Exp}	1.82	0.46	-	0.41	0.52
	M_{Calc}	1.79	0.48	-	0.48	0.37
	M_R	4.94	0.68	-	0.60	0.52
	M_T	-3.15	-0.20	-	-0.12	-0.15

$$M_T(T) = M_T(T = 5 \text{ K}) \times \frac{XMCD_T(T)}{XMCD_T(T = 5 \text{ K})}, \quad (4)$$

where the values at $T = 5$ K are determined from the magnetization measured under the same conditions by applying a two-sublattices model ($M_{Tot} = M_R + M_T$) in which the free-ion values ($\mu_R = gJ$) are assumed for the rare-earth magnetic moments. In this way the same absorption edge yields the temperature dependence of the magnetization of both sublattices $M_R(T)$ and $M_T(T)$. The result of applying this procedure is reported in Figs. 2 and 3. The total magnetization built up (Fig. 2) from the values determined from the XMCD spectra (Fig. 3 and Table 1) shows a remarkably good agreement with the experimental values of the magnetization

measured in a commercial SQUID magnetometer under the same experimental conditions (temperature and applied magnetic field). It should be noted that this remarkable agreement holds throughout both the ferromagnetic (FM) and paramagnetic (PM) regimes. Indeed, while ErFe₂ shows FM ordering from 4.2 K to room temperature ($T_C = 582$ K), the magnetic ordering temperature decreases as the Al content increases through the $R(Fe_{1-x}Al_x)_2$ series. In this way T_C is 140 K and 60 K for Er(Fe_{0.75}Al_{0.25})₂ and Er(Fe_{0.5}Al_{0.5})₂, respectively. As shown in Fig. 2, the values of the magnetization obtained from the XMCD data match well the bulk magnetization measurements at both FM and PM ordering regimes.

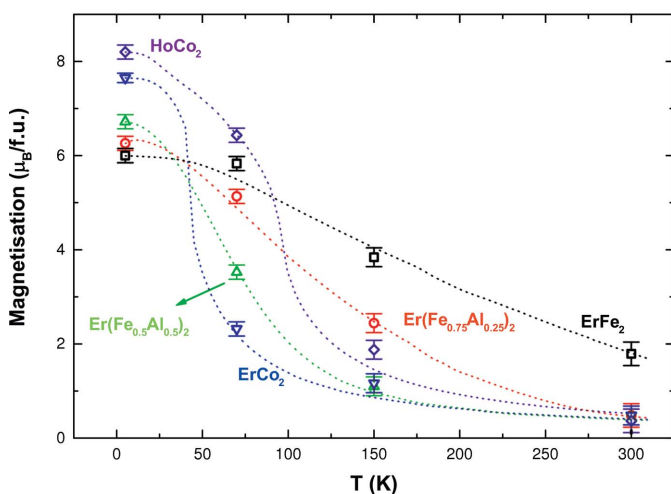


Figure 2
Comparison of the temperature dependence of the magnetization measured at 5 T by using a standard SQUID magnetometer (dotted lines) and that derived from the rare-earth L_2 -edge XMCD spectra (open symbols) in the case of ErFe₂ (black, squares), Er(Fe_{0.75}Al_{0.25})₂ (red, circles), Er(Fe_{0.5}Al_{0.5})₂ (green, triangles), ErCo₂ (blue, inverted triangles) and HoCo₂ (purple, diamonds).

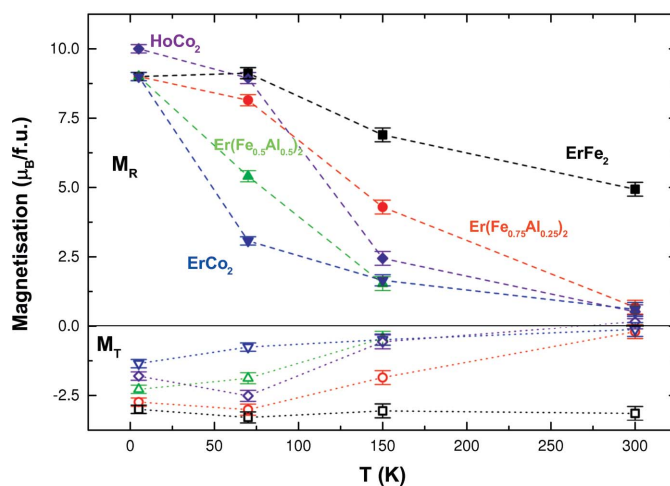


Figure 3
Temperature dependence of the magnetization of the rare-earth (solid symbols) and transition-metal (open symbols) sublattices, M_R and M_T , determined from the rare-earth L_2 -edge XMCD spectra: ErFe₂ (black, squares), Er(Fe_{0.75}Al_{0.25})₂ (red, circles), Er(Fe_{0.5}Al_{0.5})₂ (green, triangles), ErCo₂ (blue, inverted triangles) and HoCo₂ (purple, diamonds). The dotted lines are a guide for the eye.

Moreover, this method provides additional information not affordable from macroscopic tools such as the temperature dependence of both μ_R and μ_{Co} in the RCo₂ compounds. In these systems the Co 3d-band states appear near the critical conditions for the Co moment formation (Duc & Goto, 1999). The R magnetic moment is essentially constant in the whole phase diagram while the Co magnetic moment is generally thought to be developed as the rare-earth sublattice undergoes the magnetic transition. Then, the Co subsystem is magnetically ordered ($\mu_{Co} \simeq 1\mu_B$) in zero external magnetic

field owing to the effect of the molecular field, B_{eff} , created by the R moments acting on the Co sites. However, recent work calls for the existence of an intrinsic Co moment in the paramagnetic phase of ErCo₂ (Herrero-Albillos *et al.*, 2007), that opens again the debate concerning the existence or not of an intrinsic Co magnetic moment in RCo₂ systems (Duc & Goto, 1999). To date, no direct information regarding the behaviour of both R and Co sublattices can be obtained separately under the same experimental conditions. In contrast, our method fills this lack of knowledge as the

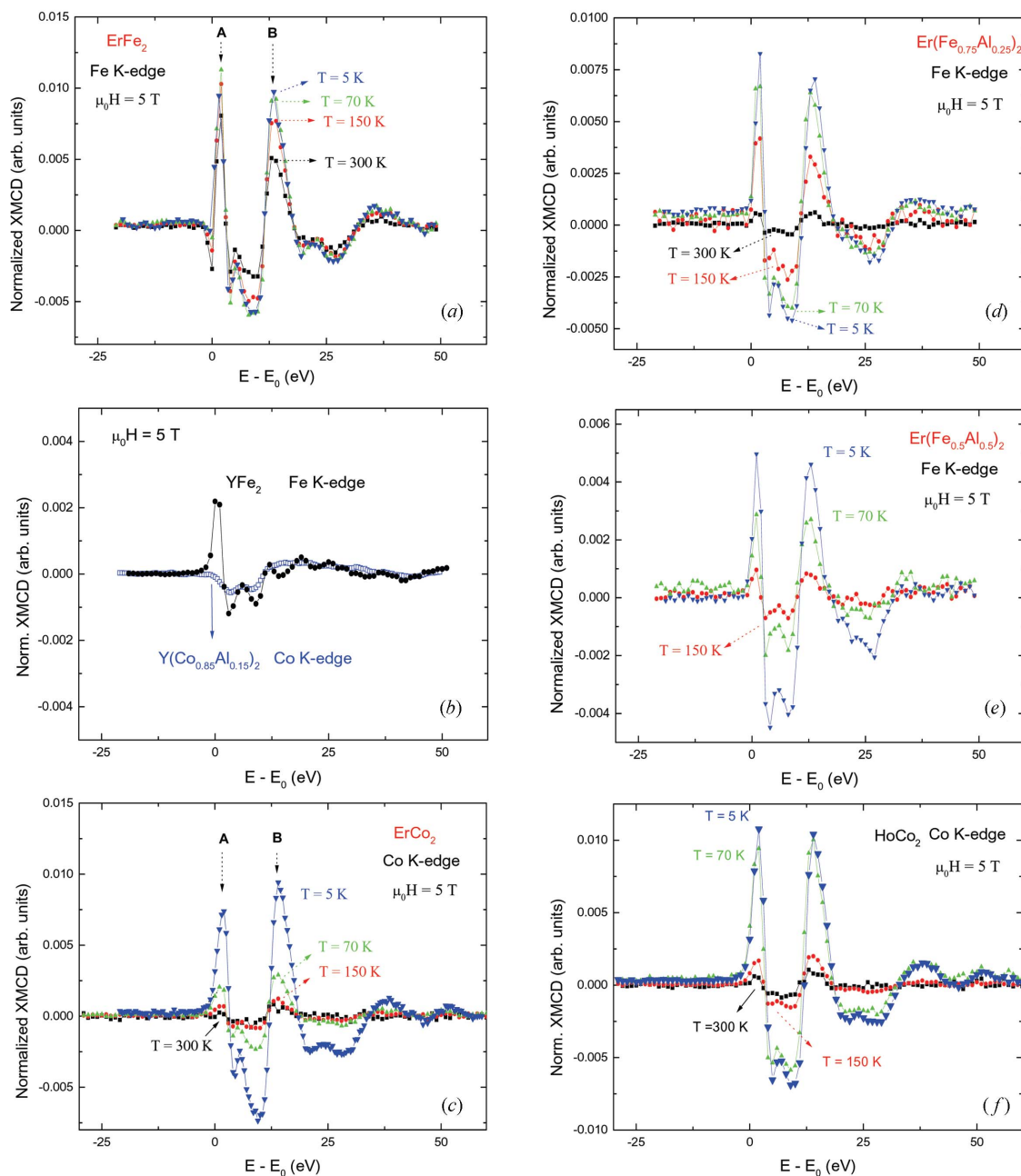


Figure 4

Temperature dependence of the normalized XMCD spectra recorded at the Fe K-edge in the case of ErFe₂ (a), Er(Fe_{0.75}Al_{0.25})₂ (d) and Er(Fe_{0.5}Al_{0.5})₂ (e), and at the Co K-edge in ErCo₂ (c) and HoCo₂ (f): $T = 5$ K (blue, inverted triangles), 70 K (green, triangles), 150 K (red, circles) and 300 K (black, squares). For the sake of completion, the Fe and Co K-edge XMCD spectra recorded at the same applied field in YFe₂ and Y(Co_{0.85}Al_{0.15})₂, respectively, are shown in panel (b).

temperature dependence of the magnetization of both sublattices $M_R(T)$ and $M_T(T)$ has been determined from the same experimental spectrum in the case of ErCo_2 ($T_C = 32$ K) and HoCo_2 ($T_C = 78$ K). As shown in Fig. 3, the magnetic ordering transition is visible in the disentangled $M_R(T)$ and $M_{\text{Co}}(T)$ curves of both ErCo_2 and HoCo_2 compounds. As shown in the figure, magnetization of the Co sublattice suddenly drops and almost disappears above T_C , in agreement with the expected destabilization of the itinerant d subsystem as the molecular field created by the R moments becomes ineffective in inducing the appearance of Co moment.

The results reported in Figs. 2 and 3 show the success in disentangling the magnetic contribution of different atomic species by using a single X-ray absorption edge. The addition of both individual sublattice magnetizations according to their ferrimagnetic coupling reproduces fairly well the temperature dependence of the macroscopic magnetization. As discussed above, the temperature dependence of the rare-earth magnetization has been derived from the modification of the intensity of the higher-energy B peak (~ 7 eV above the edge). In an attempt to confirm the validity of our results we have followed a different approach to determine $M_R(T)$. In this way we have determined this dependence by using the XMCD spectra recorded at the K -edge of the transition metal as a function of the temperature. Systematic XMCD studies performed at the K -edge of the transition metal in both R-Fe (Laguna-Marco *et al.*, 2005a; Chaboy *et al.*, 1996, 1998b, 2004, 2007c) and R-Co (Rueff *et al.*, 1998; Ishimatsu *et al.*, 2007; Chaboy *et al.*, 2007a) intermetallic compounds demonstrate that the dichroic signal measured at this absorption edge carries magnetic information not only of the T ions but also of the R ions. The influence of the rare-earth, owing to the effect of the molecular field acting on the T sites, is especially important in the case of the RFe_2 Laves phase compounds in such a way that the amplitude of the rare-earth contribution hinders the signal coming from the transition metal. This can be seen in Fig. 4 where we compare the XMCD spectra recorded at the Fe and Co edges in the compounds under study and in the cases of YFe_2 and $\text{Y}(\text{Co}_{0.85}\text{Al}_{0.15})_2$. For the Fe K -edge XMCD spectrum of YFe_2 , the XMCD spectrum closely resembles that of Fe metal (Schütz *et al.*, 1987). It shows a narrow positive peak at the absorption threshold, a ~ 12 eV-wide negative dip hindered by the presence of a small superimposed peak, and a broad positive resonance at higher energies. Despite the fact that the magnetic properties of the Fe sublattice in YFe_2 , ErFe_2 and HoFe_2 compounds are thought to be similar, their Fe K -edge XMCD spectra present noticeable differences. As shown in Fig. 4, the Fe K -edge XMCD spectrum of ErFe_2 exhibits a narrow and intense peak at the edge (A) but, in addition, a second peak of similar intensity but broader grows up at

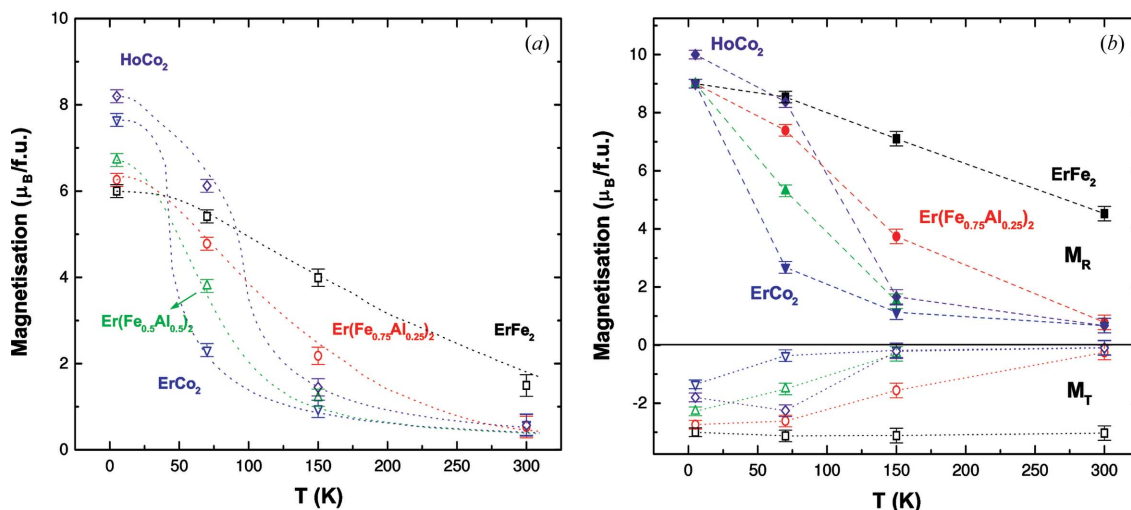
Table 2

Temperature dependence of the magnetization in an applied field of 5 T, M_{Exp} , and that derived from the XMCD spectra, M_{Calc} ; the magnetization of the rare-earth, M_R , and transition-metal, M_T , sublattices have been derived from the K -edge and L_2 -edge XMCD data, respectively.

T (K)	M ($\mu_B/\text{f.u.}$)	ErFe_2	$\text{Er}(\text{Fe}_{0.75}\text{Al}_{0.25})_2$	$\text{Er}(\text{Fe}_{0.5}\text{Al}_{0.5})_2$	ErCo_2	HoCo_2
5	M_{Exp}	6.00	6.26	6.72	7.65	8.20
	M_{Calc}	6.00	6.26	6.72	7.65	8.2
	M_R	9.00	9.00	9.00	9.00	10.00
	M_T	-3.00	-2.74	-2.28	-1.35	-1.8
	M_{Exp}	5.50	4.88	3.56	2.18	6.45
70	M_{Calc}	5.41	4.78	3.80	2.31	6.12
	M_R	8.54	7.39	5.31	2.67	8.38
	M_T	-3.13	-2.61	-1.51	-0.36	-2.26
	M_{Exp}	4.03	2.46	0.97	0.86	1.47
	M_{Calc}	3.99	2.18	1.21	0.95	1.45
150	M_R	7.10	3.74	1.51	1.13	1.66
	M_T	-3.11	-1.56	-0.30	-0.18	-0.21
	M_{Exp}	1.82	0.46	-	0.41	0.52
	M_{Calc}	1.49	0.53	-	0.59	0.57
	M_R	4.52	0.78	-	0.67	0.67
300	M_T	-3.03	-0.25	-	-0.09	-0.10

~ 15 eV above the edge. This peak was not present in the case of YFe_2 nor in Fe foil. A similar situation occurs when the Co K -edge is considered. The Co K -edge of ErCo_2 is similar to the Fe K -edge of ErFe_2 , presenting both A and B peaks. In contrast, the XMCD spectrum of $\text{Y}(\text{Co}_{0.85}\text{Al}_{0.15})_2$, similar to that of hexagonal-close-packed cobalt, presents a single negative dip. These results indicate that the magnetism of the rare-earth not only influences but dominates the spectral shape of the XMCD recorded at the transition-metal K -edge. The same behaviour is found for the whole set of compounds studied here. It is concluded from these results that the intensity of the main peaks (A and B) reflects the magnetization of the rare-earth sublattice. However, whereas both T and R contribute to the shape and intensity of peak A , only the latter is responsible for peak B . Consequently, the temperature dependence of its intensity would be a measure of the temperature dependence of the rare-earth magnetization, $M_R(T)$.

Then, we have derived $M_R(T)$ from the intensity of this peak as indicated in equation (2) and by assuming also the free ion values at $T = 5$ K for the rare-earth magnetic moments. In this way, M_R equals $9\mu_B$ and $10\mu_B$ at $T = 5$ K for the Er and Ho compounds, respectively. This dependence has been included as the factor f in equation (3). Then, we have applied again the subtraction procedure to the L_2 -edge by using this thermal dependence of the rare-earth contribution but now extracted from the transition-metal K -edge XMCD. Finally, the temperature dependence of the transition-metal magnetization has been obtained from the isolated $\text{XMCD}_T(T)$ contribution according to equations (2) and (4). The results of applying this procedure are shown in Fig. 5. As in the case of using only the L_2 data, the disentangled determination of the magnetization of both sublattices obtained from the combination of both K -edge and L_2 -edge XMCD spectra provides a good reproduction of the macroscopic magnetization data. The agreement between the $M_R(T)$ and $M_T(T)$ values derived by using both L_2 -edge (Table 1) and combined $L_2 + K$ edges


Figure 5

(a) Comparison of the temperature dependence of the magnetization measured at 5 T by using a standard SQUID magnetometer (dotted lines) and that derived by combining both the rare-earth L_2 -edge and the transition-metal K -edge XMCD spectra (open symbols) in the case of ErFe_2 (black, squares), $\text{Er}(\text{Fe}_{0.75}\text{Al}_{0.25})_2$ (red, circles), $\text{Er}(\text{Fe}_{0.5}\text{Al}_{0.5})_2$ (green, triangles), ErCo_2 (blue, inverted triangles) and HoCo_2 (purple, diamonds). (b) Temperature dependence of the magnetization of the rare-earth (solid symbols) and transition-metal (open symbols) sublattices, M_R and M_T , determined from XMCD spectra: ErFe_2 (black, squares), $\text{Er}(\text{Fe}_{0.75}\text{Al}_{0.25})_2$ (red, circles), $\text{Er}(\text{Fe}_{0.5}\text{Al}_{0.5})_2$ (green, triangles), ErCo_2 (blue, inverted triangles) and HoCo_2 (purple, diamonds). The dotted lines are a guide for the eye.

(see Table 2) methods is better than 10% over the ferrimagnetic regime for all the studied compounds. Consequently, the results presented here show the capability of this new approach to obtain the disentanglement of the magnetic contribution of different atomic species in R-T compounds by using XMCD at a single X-ray absorption edge.

4. Summary and conclusions

In this work we have reported on an XMCD study performed as a function of the temperature at the rare-earth L_2 -edge in the case of RT_2 (R = rare-earth, T = $3d$ transition metal) materials. According to previous works the analysis of the R L_2 -edge XMCD spectra shows the presence of a magnetic contribution coming from the transition metal even when the rare-earth is probed. These results show that the atomic selectivity is not lost when XMCD probes the delocalized states. On the contrary, XMCD is a simultaneous fingerprint of the magnetic contributions to the conduction band coming from the different elements in the material. Taking advantage of this peculiarity we have proposed a direct method of disentangling these contributions. As a consequence we have demonstrated that it is possible to perform element-specific magnetometry by using a single X-ray absorption edge.

This work was partially supported by a Spanish CICYT MAT2005-06806-C04-04 grant. MALM and RB acknowledge the Ministerio de Educación y Ciencia of Spain for a post-doctoral and a PhD grant, respectively. This study was performed with the approval of Japan Synchrotron Radiation Research Institute (JASRI) (Proposal No. 2005B0419).

References

- Burzo, E., Chelkowski, A. & Kirchmayr, H. R. (1990). *Landolt-Börnstein New Series Vol. III/19d2: Compounds Between Rare Earth Elements and 3d, 4d or 5d Elements*, edited by H. P. J. Wijn. Berlin: Springer-Verlag.
- Carra, P., Harmon, B. N., Thole, B. T., Altarelli, M. & Sawatzky, G. A. (1991). *Phys. Rev. Lett.* **66**, 2495–2498.
- Chaboy, J., Bartolomé, F., García, L. M. & Cibir, G. (1998a). *Phys. Rev. B*, **57**, R5598–R5601.
- Chaboy, J., García, L. M., Bartolomé, F., Maruyama, H., Marcelli, A. & Bozukov, L. (1998b). *Phys. Rev. B*, **57**, 13386–13389.
- Chaboy, J., Laguna-Marco, M. A., Maruyama, H., Ishimatsu, N., Isohama, Y. & Kawamura, N. (2007a). *Phys. Rev. B*, **75**, 144405.
- Chaboy, J., Laguna-Marco, M. A., Piquer, C., Maruyama, H. & Kawamura, N. (2007b). *J. Phys. Condens. Matter*, **19**, 436225.
- Chaboy, J., Laguna-Marco, M. A., Sánchez, M. C., Maruyama, H., Kawamura, N. & Suzuki, M. (2004). *Phys. Rev. B*, **69**, 134421.
- Chaboy, J., Maruyama, H., García, L. M., Bartolomé, J., Kobayashi, K., Kawamura, N., Marcelli, A. & Bozukov, L. (1996). *Phys. Rev. B*, **54**, R15637–R15640.
- Chaboy, J., Piquer, C., Plugaru, N., Bartolomé, F., Laguna-Marco, M. A. & Plazaola, F. (2007c). *Phys. Rev. B*, **76**, 134408.
- Chen, C. T., Idzerda, Y. U., Lin, H.-J., Meigs, G., Chaiken, A., Prinz, G. A. & Ho, G. H. (1993). *Phys. Rev. B*, **48**, 642–645.
- Duc, N. H. & Goto, T. (1999). In *Handbook on the Physics and Chemistry of Rare Earths*, Vol. 26, ch. 171, edited by K. A. Gschneidner Jr and L. Eyring. Amsterdam: Elsevier Science.
- Funk, T., Deb, A., George, S. J., Wang, H. & Cramer, S. P. (2005). *Coord. Chem. Rev.* **249**, 3–30.
- Giorgetti, C., Dartyge, E., Baudelet, F. & Galéra, R.-M. (2004). *Phys. Rev. B*, **70**, 035105.
- Harmon, B. N. & Freeman, A. J. (1974). *Phys. Rev. B*, **10**, 1979–1993.
- Herrero-Albillos, J., García, L. M., Bartolomé, F., Young, A. & Funk, T. (2007). *J. Magn. Magn. Mater.* **316**, e442.
- Ishimatsu, N., Miyamoto, S., Maruyama, H., Chaboy, J., Laguna-Marco, M. A. & Kawamura, N. (2007). *Phys. Rev. B*, **75**, 180402.
- Jo, T. & Imada, S. (1993). *J. Phys. Soc. Jpn.* **62**, 3721–3727.
- Kortright, J. B., Awschalom, D. D., Stöhr, J., Bader, S. D., Idzerda, Y. U., Parkin, S. S. P., Schuller, I. K. & Siegmann, H.-C. (1999). *J. Magn. Magn. Mater.* **207**, 7–44.

- Laguna-Marco, M. A. (2007). Editor. *A New Insight into the Interpretation of the T K-Edge and R L_{2,3}-Edges XMCD Spectra in R-T Intermetallics*. Zaragoza: Prensas Universitarias de Zaragoza.
- Laguna-Marco, M. A., Chaboy, J. & Maruyama, H. (2005a). *Phys. Rev. B*, **72**, 094408.
- Laguna-Marco, M. A., Chaboy, J. & Piquer, C. (2008a). *Phys. Rev. B*, **77**, 125132.
- Laguna-Marco, M. A., Chaboy, J. & Piquer, C. (2008b). *J. Appl. Phys.* **103**, 07E141.
- Laguna-Marco, M. A., Chaboy, J., Piquer, C., Maruyama, H., Ishimatsu, N., Kawamura, N., Takagaki, M. & Suzuki, M. (2005b). *Phys. Rev. B*, **72**, 052412.
- Lang, J. C., Srajer, G., Detlefs, C., Goldman, A. I., König, H., Wang, X., Harmon, B. N. & McCallum, R. W. (1995). *Phys. Rev. Lett.* **74**, 4935–4938.
- Lovesey, S. W. & Collins, S. P. (1996). Editors. *X-ray Scattering and Absorption by Magnetic Materials*. Oxford: Clarendon.
- Maruyama, H. (2001). *J. Synchrotron Rad.* **8**, 125–128.
- Matsuyama, H., Harada, I. & Kotani, A. (1997). *J. Phys. Soc. Jpn*, **66**, 337–340.
- Purwins, H. G., Walker, E., Barbara, B., Rossignol, M. F. & Furrer, A. (1976). *J. Phys. C*, **9**, 1025–1030.
- Rueff, J. P., Galéra, R. M., Giorgetti, C., Dartyge, E., Brouder, C. & Alouani, M. (1998). *Phys. Rev. B*, **58**, 12271–12281.
- Schütz, G., Knülle, M., Wienke, R., Wilhelm, W., Wagner, W., Kienle, P. & Frahm, R. (1988). *Z. Phys. B*, **73**, 67.
- Schütz, G., Wagner, W., Wilhelm, W., Kienle, P., Zeller, R., Frahm, R. & Materlik, G. (1987). *Phys. Rev. Lett.* **58**, 737–740.
- Stöhr, J. (1999). *J. Magn. Magn. Mater.* **200**, 470–497.
- Suzuki, M., Kawamura, N., Mizumaki, M., Urata, A., Maruyama, H., Goto, S. & Ishikawa, T. (1998). *Jpn. J. Appl. Phys.* **37**, L1488–L1490.
- Veenendaal, M. van, Goedkoop, J. B. & Thole, B. T. (1997). *Phys. Rev. Lett.* **78**, 1162–1165.
- Wang, X., Leung, T. C., Harmon, B. N. & Carra, P. (1993). *Phys. Rev. B*, **47**, 9087–9090.